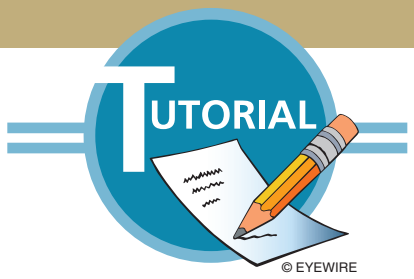

Snake-Like Robots

Machine Design of Biologically Inspired Robots

BY SHIGEO HIROSE AND HIROYA YAMADA

I (Hirose) started the biomechanical study using actual snakes and the design of snake-like robots in 1971. There were two reasons for the interest in this snake research: one is the scientific interest in the mechanism of the snake's motion and another is the engineering interest in the future applications of snake-like robots. There were already several studies on the motion of the snake; however, these were not satisfactory. The analytical method was not always consistent, and the analysis was done in somewhat artificial conditions, such as the motion of the snake in a maze with multiple pegs. So, I decided to perform a more precise analysis on standard serpentine motion. I was especially interested in the simplicity of its shape and the versatility of its function, because of its expected future applications. The simple cord-like body of the snake becomes a leg when it moves among rocks, a body when it moves from branch to branch, and a hand when it coils around a prey. From these features of the snake, I could imagine multiple applications in future. Figure 1 shows the expected applications I dreamed in those days. I used them in the oral defense of my doctor's degree dissertation in 1976. Figure 1(a) shows a downsized snake-like robot that can be utilized as an active endoscope to go into intestines. Figure 1(b) shows an active rope for a crane that automatically wraps around an object. Figure 1(c) is a polar exploration vehicle. It will glide on ice using ski blades, and the long body will enable it to cross over a crevasse. Figure 1(d) is an active hose that will approach a fire automatically using hydraulically actuated joints driven by the high-pressure water inside the hose. Figure 1(e) was drawn later for a children's book, which shows a snake-like robot that does amphibious work. From that time, I have been doing research on snake and snake-like robots, and Yamada recently joined the research group and started a renewed approach to the snake-like robots. In this article, we introduce the outline of our research so far.

In the next section, we describe the mechanism of the snake that transforms the muscular force of the body into a thrusting force. We also discuss some of the aspects of snake locomotion and estimate the required power for serpentine motion. In the "Mechanical Designs of Snake-Like Robots" section, we classify the snake-like robots that we have developed so far and describe their mechanical design. Finally, in the "Conclusions" section, the future direction of the development of snake-like robots is discussed.

Digital Object Identifier 10.1109/MRA.2009.932130

Kinematics of Snake Motion

Kinematic Models and Basic Equations of the Snake

The movement of a snake can be categorized into the following four types: 1) serpentine movement, 2) rectilinear movement, 3) concertina movement, and 4) side winding movement. Out of these, the serpentine movement is the most smooth and obviously effective mode of locomotion, and it is widely observed in almost all species of snakes; therefore, our research started with the analysis of serpentine movement.

Figure 2 shows a skeleton model of part of a snake's body, consisting of serially connected links with length δs. The links are supposed to make contact with the ground only at the joints, and a bending torque T_i is generated by the muscles at the joint P_i $(i = 1, 2, \ldots)$. The torque T_i applies forces f_i to the ground from joints P_i. The resultant forces f_{ti} acting along the body's tangential direction [the direction that bisects θ_i as

1070-9932/09/$25.00©2009 IEEE

Authorized licensed use limited to: IEEE Xplore. Downloaded on November 21,2023 at 09:26:57 UTC from IEEE Xplore. Restrictions apply.

shown in Figure 2(b)] and the normal force f_{ni} acting normal to the tangential force can be obtained as follows:

$$f_{ti} = \{(f_i - f_{i-1}) + (f_{i+1} - f_i)\} \sin\frac{\theta_i}{2} \simeq \frac{T_{i+1} - T_{i-1}}{2\delta s}\theta_i, \quad (1)$$

$$f_{ni} = \{(f_{i+1} - f_i) - (f_i - f_{i-1})\} \cos\frac{\theta_i}{2} \simeq \frac{T_{i+1} - T_i}{\delta s} - \frac{T_i - T_{i-1}}{\delta s}. \quad (2)$$

Here, as the snake's links (bones) are so short, we can assume $\delta s \to 0$. Then, all the relations can be expressed in the form of differential equations, by substituting θ_i for the curvature $\kappa(s) = \theta_i/\delta s$ and $T_i \to T(s)$, $f_{ti} \to f_t(s)\delta s$, and $f_{ni} \to f_n(s)\delta s$. In this way, the following equations can be derived:

$$f_t(s) = \frac{dT(s)}{ds}\kappa(s), \quad (3)$$

$$f_n(s) = \frac{d^2T(s)}{ds^2}. \quad (4)$$

In these equations, the parameter s indicates the position of the body measured along the body from the head. Additionally, $T(s)$ indicates the bending torque, $\kappa(s)$ indicates the curvature, $f_n(s)$ indicates the force per unit of length that acts on the ground in the normal direction, and $f_t(s)$ indicates the force per unit length that acts on the ground in the tangential direction. Equations (3) and (4) indicate the relationship between the torque, curvature, and forces that are applied to the ground, so that it shows the basic principle of the mechanism of a snake's locomotion. In [1], an overall analysis of the snake's locomotion is done based on these basic equations.

Just recently, however, Yamada found that these basic equations were incomplete because the axial force acting inside the link is not considered. This force can be neglected if the thrusting force generated at a joint is balanced by the resistive force acting on the same joint from the ground. But this assumption is not valid if the snake lifts a part of its body from the ground. Yamada derived more generalized equations by using the study of elastica in 19th century as follows [2]:

$$F_t'(s) = F_n(s)\kappa(s) + f_t(s), \quad (5)$$

$$F_n'(s) = -F_t(s)\kappa(s) - f_n(s), \quad (6)$$

$$T'(s) = -F_n(s). \quad (7)$$

Here, $F_t(s)$ and $F_n(s)$ are newly added internal forces. $F_t(s)$ indicates the force toward the body axis, and $F_n(s)$ indicates the force toward the direction perpendicular to the body axis as shown in Figure 3. If the internal axial force is assumed to be zero, $F_t(s) = 0$, and this assumption is assigned to (5)–(7), which in turn correspond to (3) and

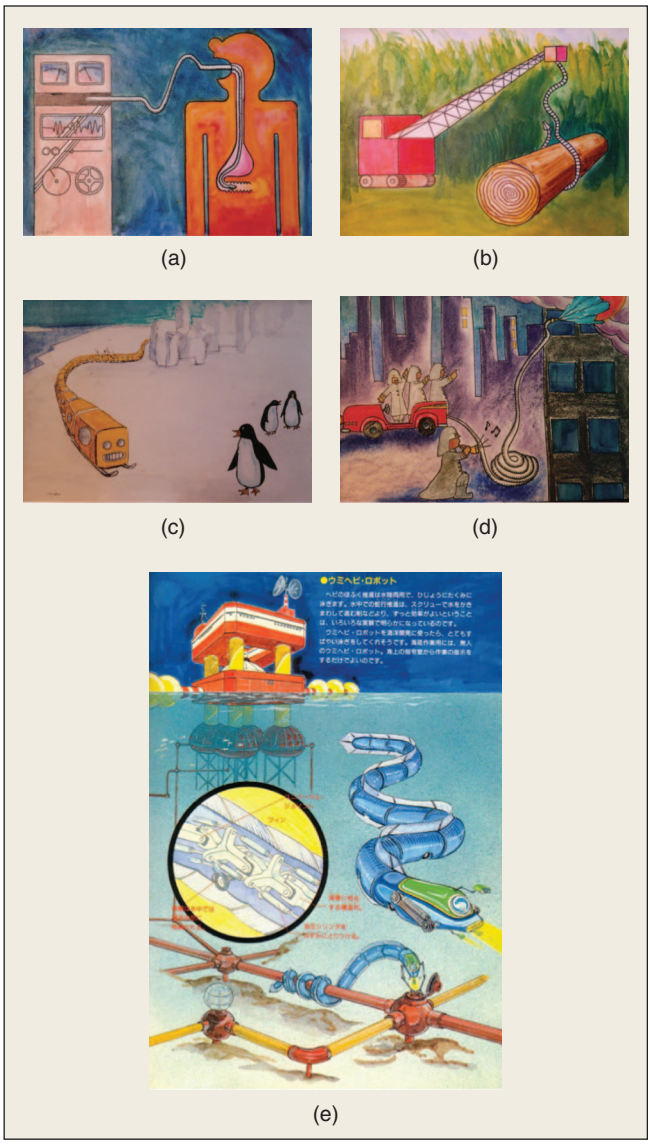

Figure 1. *Expected applications of snake-like robots. (a) Active endoscope. (b) Active rope. (c) Polar exploration vehicle. (d) Active hose. (e) Amphibious snake-like robot.*

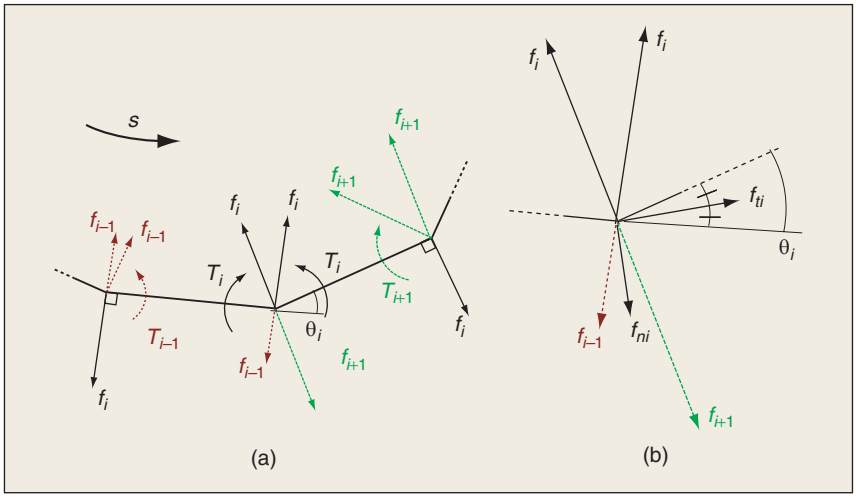

Figure 2. *Forces and torque in skeleton model. (a) Generated forces at joints. (b) f_{ni} and f_{ti}.*

Authorized licensed use limited to: IEEE Xplore. Downloaded on November 21,2023 at 09:26:57 UTC from IEEE Xplore. Restrictions apply.

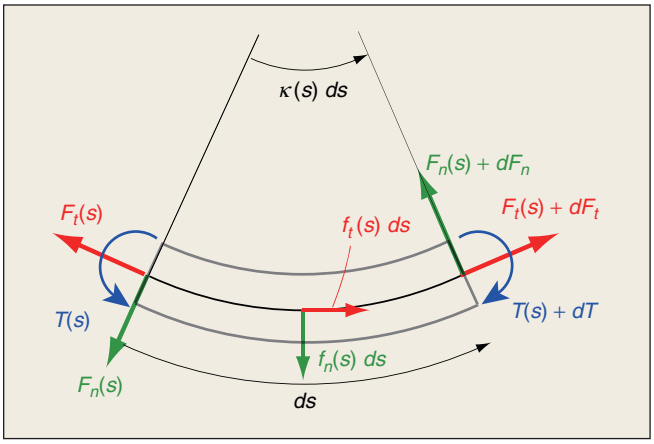

Figure 3. *Forces and torque in continuous model.*

(4). Equations (5)–(7) can also be derived by applying additional internal axial forces $F_t(s)$ in Figure 2.

Morphology of Creeping Motion

To analyze the creeping motion, a standard body-shape curve that is formed in a typical serpentine motion should be clarified. The shape of the curve may be influenced by many factors. Among them, we assumed that the smoothness of the snake's muscle motion is the most dominant factor. Based on this assumption, we proposed the curve shown in Figure 4. The main feature of this curve is that the curvature changes along the body axis s in a sinusoidal manner, as shown in the following equation [1]:

$$\kappa(s) = -\frac{2\pi\alpha}{L}\cos\left(\frac{2\pi}{L}s\right). \tag{8}$$

Here, $s = 0$ is the starting point of the curve and corresponds to the first point P on the left side of the curve. The parameter α is the angle of the body at point O relative to the traveling direction (called the winding angle), and L is the length (wavelength) of the curve in one cycle of the curve. We once magnified the figures of the real snakes' gliding motion and compared them with the assumed curves with the same winding angle α and body length L and found out that they agreed with the theoretical curves very well. Given this fact, we called this curve as serpenoid curve and used it for analysis.

Forces Acting Along the Body

By using the basic equations (5)–(7) and the assumption of the serpenoid curve, we can analyze the forces acting along the body. We add some more assumptions: 1) the frictional force in the tangential direction is assumed to be constant as $f_t(s) = C$, 2) muscular force distribution along the curve is sinusoidal. From the fact that the muscular force should be zero at the point P where the direction of body bending changes and the maximum force should be generated at point O where the muscle reaches its natural length, it is expressed as follows:

$$T(s) = -T_{mo}\sin\left(\frac{2\pi}{L}s\right). \tag{9}$$

If we substitute this equation into (5)–(7) and integrate, the following equations can be obtained. In the integration procedure of (5), we consider the condition that the tangential internal force that acts on the body should be periodic and obtain the following equation:

$$\frac{2\pi^2\alpha T_{mo}}{L} = CL. \tag{10}$$

The right-hand side of (10) indicates the sum of the frictional resistance acting along the body, while the left-hand side indicates the sum of the propulsive force generated by the bending torque of the muscle. From (6), the distribution of the normal force of the body against the ground can be expressed as follows:

$$f_n(s) = \frac{C}{\alpha}\sin\left(\frac{2\pi}{L}s\right)\left\{2 - \frac{\alpha^2}{2}\left(1 + \cos\left(\frac{4\pi}{L}s\right)\right)\right\}. \tag{11}$$

In Figure 5, the derived force distribution along the snake's shape is illustrated. From this analysis, we find that the snake shows a tendency to push against the ground most significantly around the point O. The forces acting around each point O are not parallel to the traveling direction of the snake, but since they oppose each other every half cycle, the net normal forces will be directed in the traveling direction, and these normal forces push the snake's body forward. This motion of the snake is somewhat similar to ice skating. In ice-skating motion, people will kick the ice most when the shoe blade is set at an angle largest to the direction of motion.

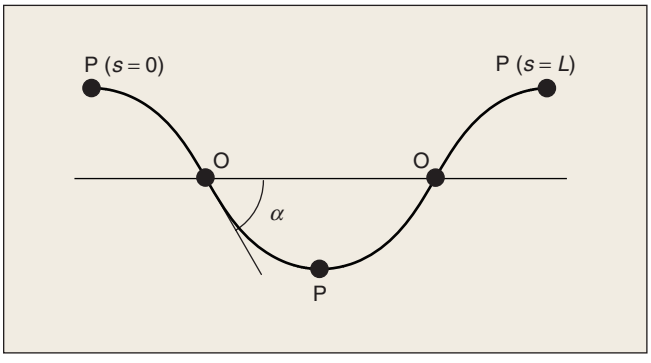

Figure 4. *Serpenoid curve.*

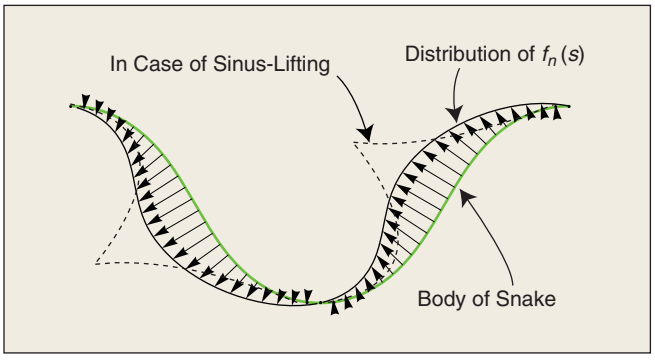

Figure 5. *Distribution of normal force.*

Authorized licensed use limited to: IEEE Xplore. Downloaded on November 21,2023 at 09:26:57 UTC from IEEE Xplore. Restrictions apply.

We once attached an electromyography sensor to measure the muscular force and used a specially made force sensor to measure the normal force at a part of a snake while it moved around. From this experiment we found the normal force distribution of a real snake. The measured normal force distribution of the real snake is shown by the dotted line of Figure 5. It tends to be concentrated around the point P, especially when the snake moves fast. From this discovery, the authors were able to explain a very interesting habit of the snake. This habit is to lift a part of the body as shown in Figure 6 when moving fast. The snake lifts the body around points P and contacts the ground only around points O. There has been no proper explanation for the cause of this habit of the snake earlier, but I found that this habit is one of the by-products of the serpentine motion that maximizes locomotion efficiency. As shown in Figure 6, the normal force tends to concentrate around points O when the snake moves fast, and if the snake moves like this, the body segments around points O tend to slip because of the large normal force produced in this area. Therefore, we can interpret the habit of the snake shown in Figure 6 as a result of the snake's effort to prevent slippage of the body at points O, because the weight of the body can be concentrated at the points O by lifting the body around points P. This is how I explained the habit of the snake, and I named the specific gliding motion as sinus lifting. Recently, we have again started to notice the importance of sinus-lifting motion, because it is effective in driving snake-like robots over ground with high friction, such as a soft carpet.

Required Power for Serpentine Motion

The torque and angular velocity of a joint reaches its maximum at points O, and thus estimation of the maximum required power can be calculated at points O as follows. From (10), the maximum torque at point O is expressed as follows:

$$T_{mo} = \frac{CL^2}{2\pi^2\alpha}. \tag{12}$$

From (8), the angular velocity of the joint rotation is expressed as follows:

$$\omega = \frac{\partial\kappa(s)}{\partial s} l v = \frac{4\pi^2\alpha l v}{L^2} \sin\left(\frac{2\pi}{L} s\right), \tag{13}$$

where l is the length of the joint and v is the velocity of the body of the snake. Therefore, the maximum required power should be produced at point O, and it can be obtained from the products of (12) and (13) as follows:

$$W_{\max} = 2Clv = 2\mu_t m_l g v. \tag{14}$$

Here, μ_t is the frictional coefficient in the body's axial direction, m_l is the mass of a joint, and g is the gravitational acceleration. For example, if you want to design a snake-like robot with weight $m_l = 0.5$ kg and have a body with frictional coefficient $\mu_t = 0.1$ that is driven at a velocity $v = 1$ m/s, the required power can be calculated as $W_{\max} = 0.98$ W.

Mechanical Designs of Snake-Like Robots

Classification

A snake-like robot is basically composed of a number of serially concatenated joints. Here, the major snake-like robots developed by the authors are introduced and classified into five different types:

1) active bending joint type
2) active bending and elongating joint type
3) active bending joint and active wheel type
4) passive bending joint and active wheel type
5) active bending joint and active crawler type.

Active Bending Joint Type

The active bending joint type, which consists of serially connected active bending joints, is the most standard form of a snake-like robot.

Active Cord Mechanism-III

I developed ACM-III (Figure 7) in 1972, and this was successful in demonstrating the world's first serpentine motion by using the same locomotion principle of a real snake. The ACM-III was 2 m in total length and 28 kg in weight and

Figure 6. *Sinus lifting.*

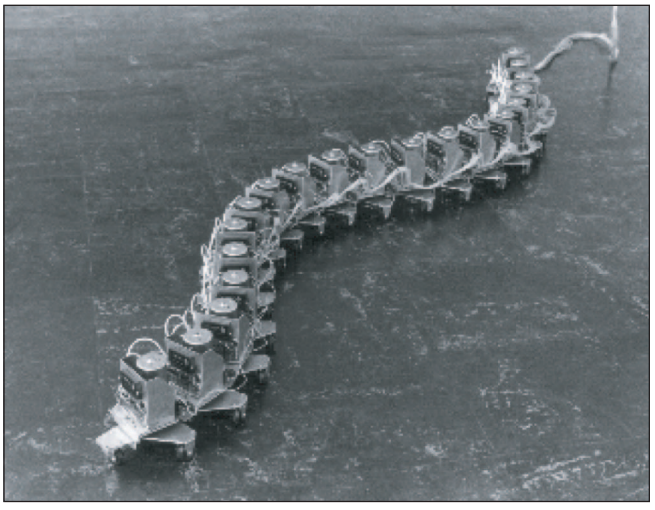

Figure 7. *ACM-III.*

Authorized licensed use limited to: IEEE Xplore. Downloaded on November 21,2023 at 09:26:57 UTC from IEEE Xplore. Restrictions apply.

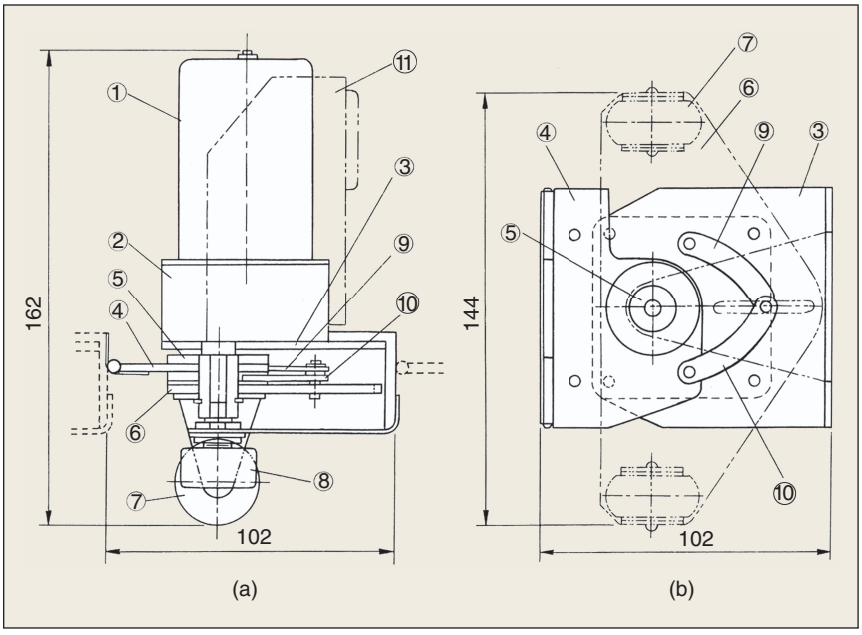

Figure 8. *Schematic diagram of ACM-III. (a) Side view. (b) Bottom view.*

consisted of 20 connected joints that generated swinging motion around vertical axes. Figure 8 shows a joint mechanism of ACM-III. The motor (1) and reduction gear (2) are mounted on a board (3), and another board (4) is rotated relative to board (3). The potentiometer (8) measures the rotation angle to form a servomechanism. Castors are attached to the plate (6), which are mechanically restricted to direct the intermediate angle between the boards (3) and (4). This mechanism to regulate the direction of the casters is introduced to realize the same kinematic condition of Figure 2, where the direction of the joint motion is made to follow the bisecting angle of the joint θ_i, and the frictional coefficient is small in the tangential direction and large in the normal direction. ACM-III has a joint mass of $m_l = 1.4$ kg, and the castor's friction coefficient $\mu_t = 0.034$. Therefore, to produce serpentine motion with velocity $v = 0.5$ m/s, the required power can be calculated as $W_{\max} \approx 0.47$. W by (14). The rated power of the joint actuator of ACM-III is 10 W, and the machine is designed to be sufficient for normal serpentine motion.

Figure 9. *ACM-R3.*

ACM-III realized a smooth creeping motion by transmitting the bending signal for the joint servomechanism from front to rear, where the velocity reached 0.5 m/s. In addition, we also conducted shape following control with ACM-III by adding tactile sensors on both sides of the body. It was implemented using limit switches and special signal processing circuits. As a result of this implementation, we were able to realize a movement, where a robot automatically wraps around an object. For this motion, we introduced a kind of neural network control that corresponds to the lateral inhibition of animals' nervous systems. By combining this neural network control of lateral inhibition and the shifting control signal of the joint servomechanism from front to rear, we could also realize an autonomous driving experiment where the ACM-III moved inside a maze.

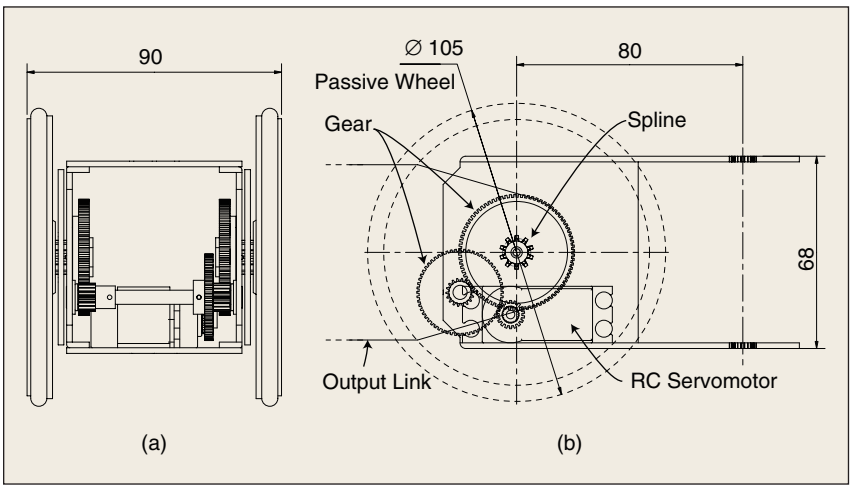

Figure 10. *Schematic diagram of ACM-R3n. (a) Back view. (b) Side view.*

ACM-R3

The ACM-R3 [3] (Figure 9), developed in 2001, is a wireless-type snake-like robot that can perform three-dimensional (3-D) motion. This robot is composed of 20 joints, and it is 1.8 m in length and 12 kg in weight. This robot is composed of two types of bending joints, having different bending axes connected alternately at 90°. This connection makes it possible to make 3-D motion. Because each joint drives 1 degree of freedom (DoF), the driving mechanism can be simple, and this shape became the standard of 3-D snake-like robots [4].

Figure 10 shows the internal mechanisms of the joint of ACM-R3n, a modified

Authorized licensed use limited to: IEEE Xplore. Downloaded on November 21,2023 at 09:26:57 UTC from IEEE Xplore. Restrictions apply.

model of ACM-R3. The bending motion is generated by a radio-controlled (RC) servomotor with an additional double-stage reduction gear, with a reduction ratio of 1:15 to increase the output torque up to 15 N·m. A nickel–hydrogen (7.2 V, 1.6 Ah) battery is installed in the ACM-R3, and it allows the robot to operate continuously for more than 2 h.

In the previous model of ACM-III, we introduced a mechanism to direct the passive wheels to the bisecting angle of the connecting joints to realize the same condition of Figure 2. In the ACM-R3 and ACM-R3n, we detached this half-angle mechanism and, instead, simply attached the wheels at the middle of the joints as shown in Figure 11. This mechanism is simpler and can correspond to Figure 2, only by reconsidering the location of joint P_i to be the central point between passive wheels. The passive wheels of ACM-R3 are attached on both sides of the active joints, and their diameter is made larger than the profile of the link. This configuration gives the following advantages: 1) a wide movable angle of the bending joint, 2) the wheels fully cover the body regardless of the posture of ACM-R3; this enables the body to slide smoothly regardless of its posture, and 3) smooth, low-friction rotation of the wheels even on high-friction ground.

ACM-R3 can perform creeping motion at a maximum speed of about 1 m/s, and it can also lift its neck up to about 500 mm. Additionally, this robot can perform 3-D motions such as side winding and sinus lifting, so that it has proven performance as a research platform for terrestrial snake-like robots. Recently, we added contact sensors on the front segment and succeeded in demonstrating terrain adaptive motion to go over obstacles of about 100 mm in height, as shown in Figure 12.

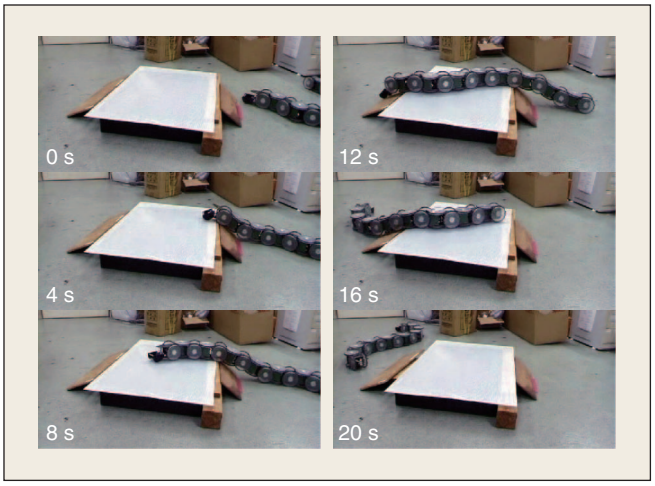

Figure 12. *Motion of ACM-R3n.*

ACM-R5

ACM-R5 [5] is an amphibious snake-like robot characterized by its hermetic dust- and waterproof body structure. A similar model named HELIX [6] was made in 2001, and ACM-R5 is the modified model of HELIX. To realize the hermetic structure, a universal joint mechanism driven by a pair of geared motors from both ends is introduced. The external parts of these universal joint mechanisms are sealed by flexible bellows and an aluminum outer shell. The number of connecting joints can be changed; the robot shown in Figure 13 is composed of eight joints, 1.6 m long and with a weight of 6.5 kg.

The joint part, as shown in Figure 14, is composed of the motor and reduction gears that drive the universal joints, along with the bellows and outer shell to cover them. When we designed this structure, we paid special attention to the fact that the universal joint cannot transmit constant-velocity rotation when the connecting shaft is not coaxial or is inclined. However, the bellows that cover the universal joint can transmit constant-velocity rotation regardless of the angle of the connecting shaft, and thus there is a discrepancy between these transmission mechanisms. To solve this problem, we introduced a passive rolling axis at the connecting member of the center of the universal joint. The driving motor is the same as that of ACM-R3, and the reduction ratio of the gear train is 7.5:1.

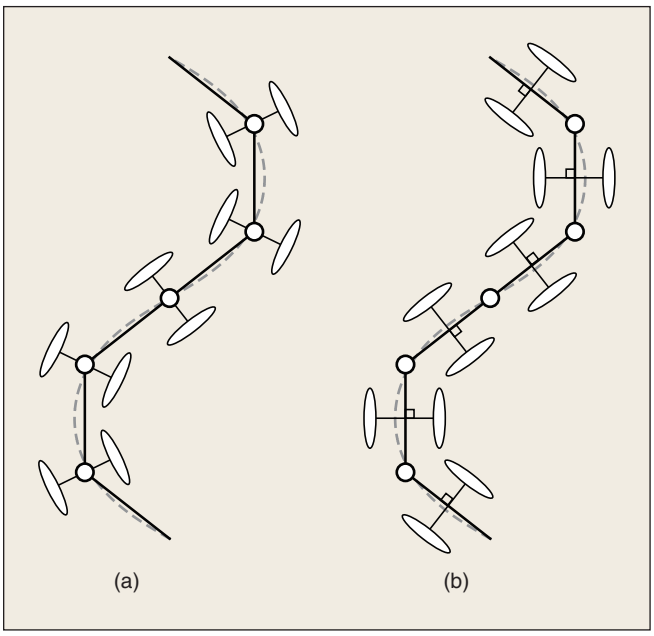

Figure 11. *Position of passive wheels. (a) ACM-III. (b) ACM-R3.*

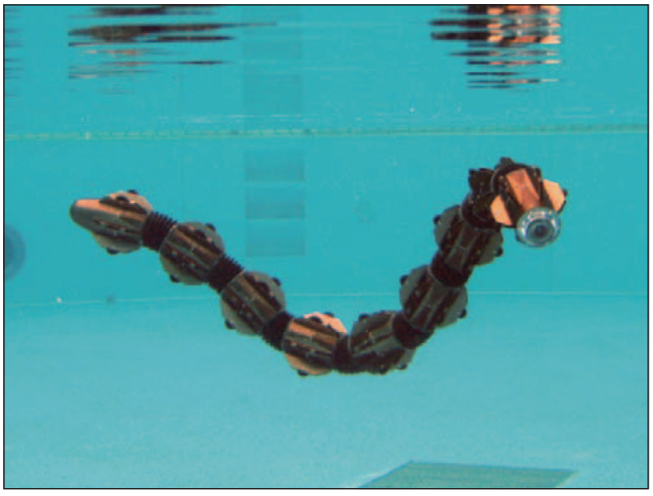

Figure 13. *ACM-R5.*

Authorized licensed use limited to: IEEE Xplore. Downloaded on November 21,2023 at 09:26:57 UTC from IEEE Xplore. Restrictions apply.

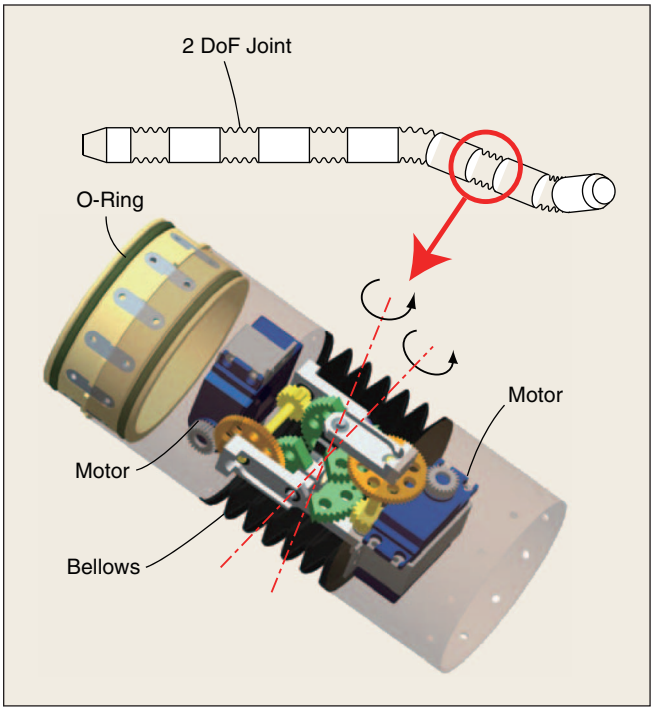

Figure 14. *Joint of ACM-R5.*

Joints are designed to be connected with a polyacetal tube, and an O-ring fitted in the tube's groove keeps out water.

Underwater swimming fins are attached around the outer circumference of the ACM-R5, and passive wheels are also attached to the tip of each fin to allow creeping motion on the ground. With these fins and wheels, the ACM-R5 can perform propulsive motion at a speed of about 0.4 m/s on the ground as well as in water. The specific gravity of the robot's body is almost the same as that of water (actually a little bit lighter than water), which makes it possible to swim in water quite smoothly. We believe that the age of amphibious snake-like robot was opened by this ACM-R5.

Figure 15. *Slim Slime robot.*

Active Bending and Elongating Joint Type

When the freedom to elongate is given to a snake-like robot, the robot can exhibit motion like a worm. This motion makes it possible to have forward movement while maintaining a straight body form, so that the robot can move through a straight pipe where creeping motion is impossible to perform. Focusing on these features, we have developed the following snake-like robots with joints that can bend and elongate at the same time.

Slim Slime Robot

The Slim Slime robot [7] (Figure 15) is a robot made up of linearly connecting multiple modules that pneumatically bend and elongate. Inside a module (Figure 16), three metal bellows are arranged in parallel at regular intervals with an identical circumference. Both ends of each bellows are fixed with two disks, and the disks are connected to each other by expanding springs. These bellows elongate when compressed air is supplied, and they shrink when the air is drained out. Each bellow has two solenoid valves embedded, used for the intake and expulsion of the compressed air. The module bends and elongates by controlling the compressed air that is supplied to the three bellows. The module is 128 mm in diameter, from 114 to 178 mm in length, 1.7 kg in weight, and has a maximum bending angle of 30°.

The Slim Slime robot shown in Figure 15 is composed of six connected modules, from 730 to 1,120 mm in length and 12 kg in weight. The Slim Slime robot has realized a wide variety of movement styles by bending and elongating. This robot has also succeeded in performing locomotion in an inclined pipe as illustrated in Figure 17.

ACM-S1

ACM-S1 [8] (Figure 18) is another type of snake-like robot, which has joints that bend and elongate. The ACM-S1 is composed of three joint sections, and it is 0.9 m in length and 3.7 kg in weight. The significant mechanism of the ACM-S1 was in its

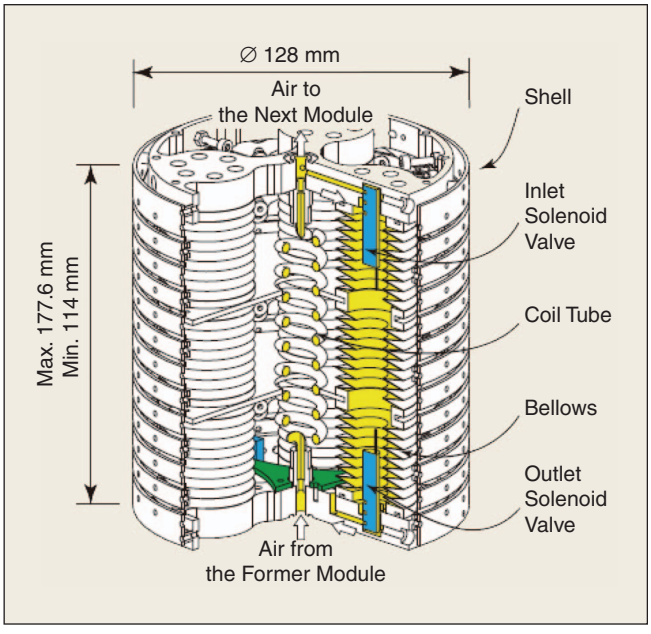

Figure 16. *Module of Slim Slime robot.*

Authorized licensed use limited to: IEEE Xplore. Downloaded on November 21,2023 at 09:26:57 UTC from IEEE Xplore. Restrictions apply.

bending and elongating part. Instead of pneumatic bellows, ACM-S1 introduced an elastic rod driving mechanism as shown in Figure 19. At the base of each joint, three linear drive mechanisms using slide screws are arranged at regular intervals with an identical circumference, and one end of an elastic rod (urethane rubber) is fixed to each of them. The other end of the elastic rod is fixed to the other side of the joint. This joint bends and elongates by controlling the length of the three elastic rods. The key technology to design this mechanism is the selection of elastic rods with the proper elasticity, and we selected the best one after several bending experiments. All the joints are covered with bellows so that the robot is waterproofed. Motion control was conducted by approximating the joint's bending form of the elastic rod by a circular arc and calculating the displacement of the linear actuators to realize the target joint form.

With the current design, ACM-S1 has wheels that roll only in one direction only because of the effect of one-way clutch so as to perform effective motion. Because of these wheels, the ACM-S1 can gradually push out its body to move ahead by periodically elongating the joints. In addition, this robot can change direction by elongating its joints while also controlling the bending form of its joints (Figure 20). To put this robot to practical use, it is essential to develop a device that contacts the ground and functions in the same way as the one-way clutch but having higher dust resistance.

Active Bending Joint and Active Wheel Type

ACM-R4

It is also desirable to have snake-like robots that can move in environments like pipes that have long straight narrow sections and also bent sections. The introduction of bending and elongating joints is one of the solutions, but adding active wheels can also solve the problem. The snake-like robot ACM-R4 [9] (Figure 21) has active joints and active wheels and was developed based on such a perspective. This robot consists of nine joint sections, and it is 1.1 m in length and 9.5 kg in weight.

As in the case of ACM-R3n, the ACM-R4 was also developed by connecting joints whose bending direction differed

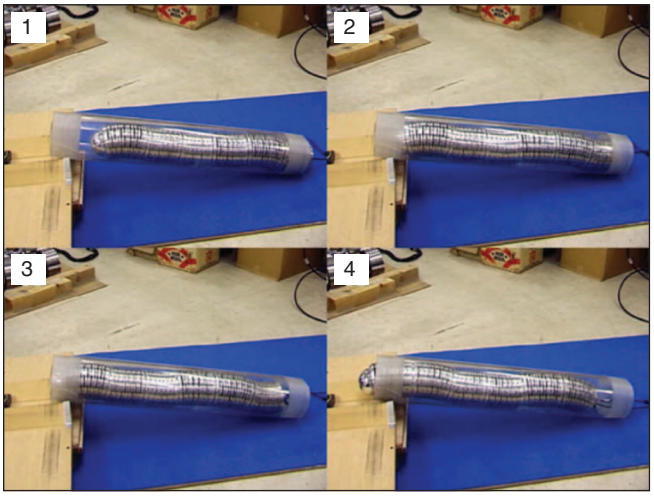

Figure 17. *Locomotion in an inclined pipe.*

The serpentine movement is the most smooth and obviously effective mode of locomotion.

by 90° alternately. The active wheels were attached to the same axes where the passive wheels of ACM-R3 were attached. This arrangement is superior to attaching large bore wheels

Figure 18. *ACM-S1.*

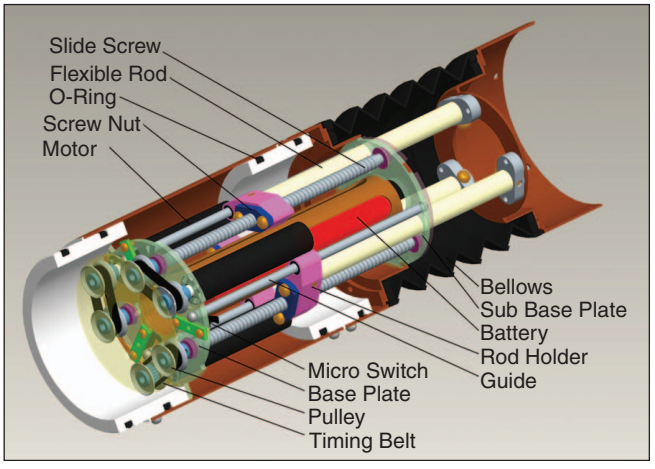

Figure 19. *Joint of ACM-S1.*

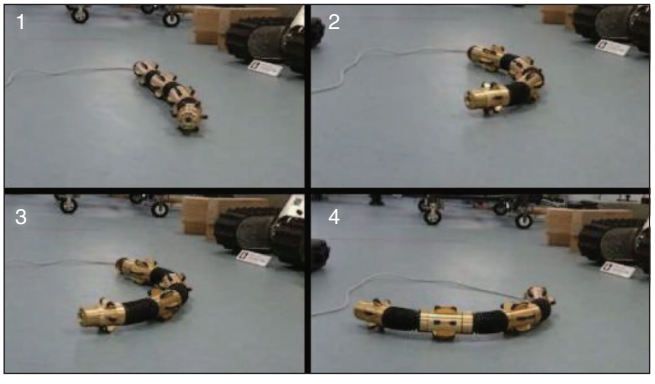

Figure 20. *Steering motion of ACM-S1.*

Authorized licensed use limited to: IEEE Xplore. Downloaded on November 21,2023 at 09:26:57 UTC from IEEE Xplore. Restrictions apply.

without interfering with the joint rotation around the axes. We sealed the rotational axes using V-rings to make it water- and dustproof.

Inside each joint, the motors that drive the joint and the wheels are housed (Figure 22). To provide space inside, a four-point contact bearing with a large diameter is used for the joint's rotation axis, and the joint is driven by internal gears. A long and thin snake-like robot tends to be very vulnerable if a large torque is applied to certain joints when a part of the body is lifted, so we introduced a torque limiter in the joint's bending drive system. It is made from a rubber ring between the internal gears on the final stage of the drive system and the joint frame. ACM-R4 could move in a straight form, so that it can move through a narrow pipe that bends at a right angle (Figure 23). In addition, this robot has a great ability to go over obstacles when compared with other type of robots with passive wheels.

Passive Bending Joint and Active Wheel Type

Genbu

Snake-like robots are characterized by their ability to actively bend the body to adapt to rough terrain. However, in the case where no large gap exists or the terrain is markedly uneven in the environment where a robot moves, the robot moves more easily not by actively bending its body but by passively changing the body shape among obstacles while the propulsive force is generated by wheels. The Genbu [10] of Figure 24 was developed based on such perspective.

The Genbu is characterized by a structure that has a number of large-diameter active wheels attached to the body connected by passive rubber joints. All the wheels are independently driven, and the propulsive force of each wheel is transmitted through the elastically joined body. Steering can

Figure 21. *ACM-R4.*

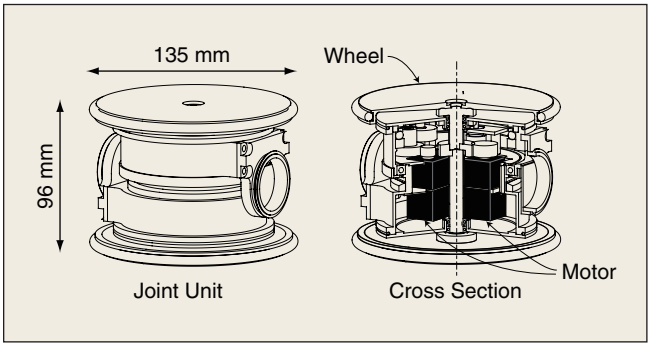

Figure 22. *Structure of an unit of ACM-R4.*

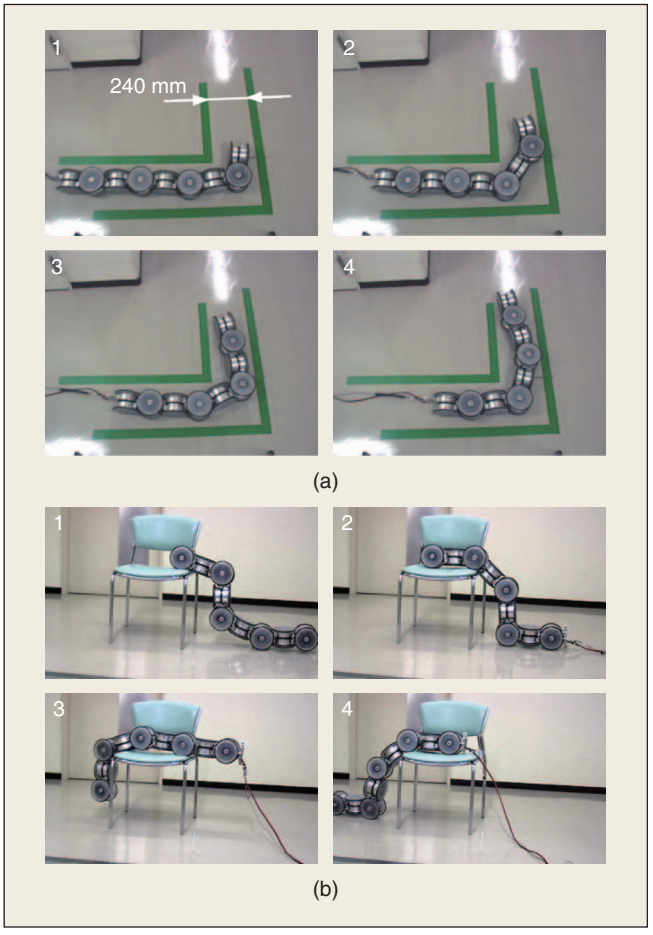

Figure 23. *Motion of ACM-R4. (a) Corner. (b) Climbing a step.*

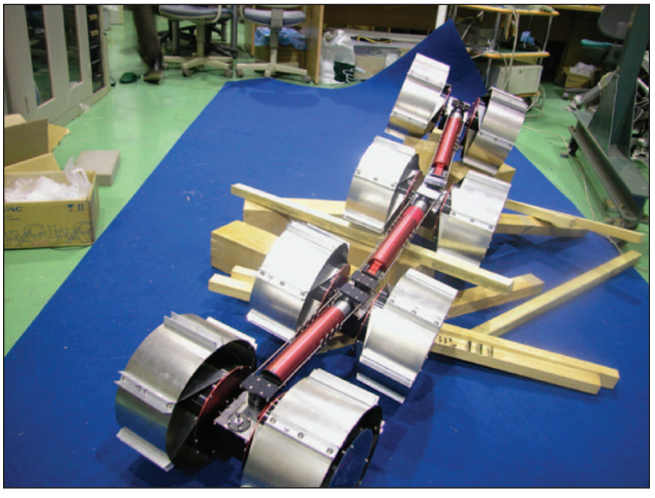

Figure 24. *Genbu.*

Authorized licensed use limited to: IEEE Xplore. Downloaded on November 21,2023 at 09:26:57 UTC from IEEE Xplore. Restrictions apply.

be performed by properly adjusting the propulsive forces generated by the wheels so as to change the bending direction of the entire body. The body can passively adapt to rough terrain, so that any unnecessary force does not affect the body even when the robot moves at higher speeds. This gives the body a high degree of toughness and durability.

The Genbu-III shown in Figure 24 is 1,700 mm in length, 400 mm in width, and 35 kg in weight, and incorporates all the necessary circuits such as a battery and motor driver. This robot has succeeded in going over an obstacle exceeding the wheel's diameter by means of effective passive joints and multiple active wheels (Figure 25).

Active Bending Joint and Active Crawler Type

Souryu

Souryu was developed with the goal of putting snake-like robots into practice as rescue robots, which can conduct search operations among the debris of collapsed buildings when a huge earthquake strikes. The characteristic of a snake-like robot is its slender and long body with active joints; however, when considering the usage of the robots in such a disaster area, we should select a simple mechanism while maintaining the features of the snake-like slender and active body. With this in mind, the body segments used for Souryu are limited to three, and each segment is covered with crawlers so that the propulsive force can be transmitted no matter how the crawlers come in contact with the rubble. The joints connecting the segments can be bent in two directions by a pair of prismatic links.

Six types of Souryu robots have been developed in the past. Figure 26 shows one of them, Souryu-IV [11]. The Souryu-IV is 1,210 mm in length, 160 mm in width, 132 mm in height, and 11.9 kg in weight. It is composed of three segments, with crawlers connected with bending joints. The bending joint (Figure 27) is composed of a pair of parallel link mechanisms that are driven by slide screws. The right-handed screw and left-handed screw are set on both ends of the slide screw's shaft, so that the robot can perform a symmetrical bending motion at the anterior or posterior connection parts simultaneously. A compact mechanism is used to drive the joint with only two motors, so that each vehicle is connected without limiting the space for the drive mechanism of the crawlers. By using active joints, this robot can steer, go over obstacles, and change its body position along the roll axis (Figure 28). Television (TV) cameras are attached to the body, and they send information about the surroundings to the robot operator.

For the crawler of Souryu-IV, we specially developed a light weight and rugged unit consisting of a strong steel belt with a rubber grouser glued on its surface and light-weight plastic pulleys. This belt unit has fringe rubber projections on the rim of both sides, and it has slide-on covering plates on the side of the crawlers to prevent fiber-type rubble entering into the belt and pulleys. This protection mechanism is especially important, because fiber-type rubbles

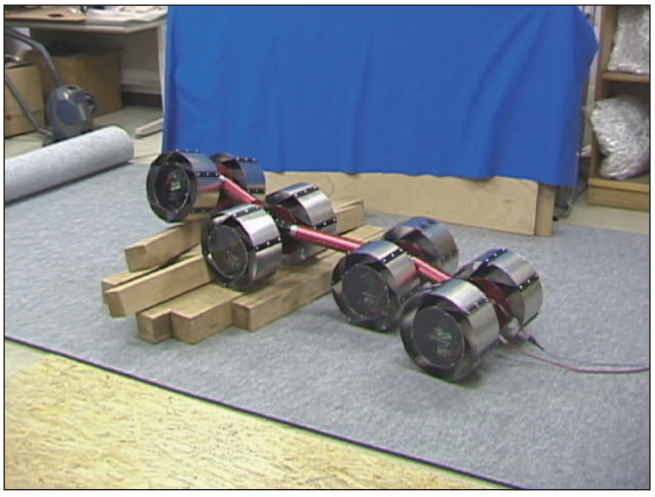

Figure 25. *Going over rough terrain.*

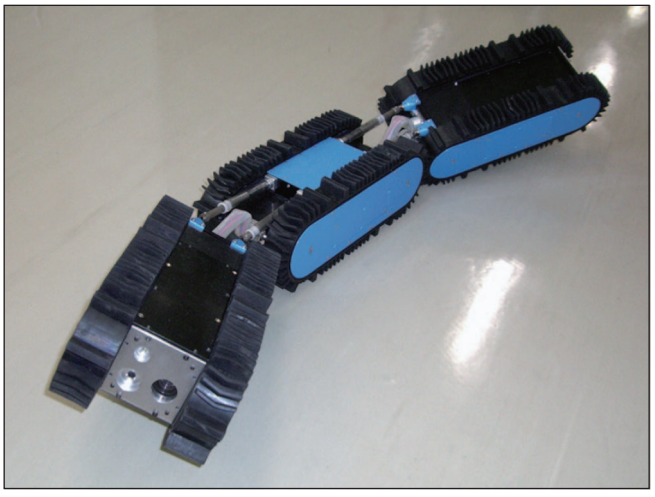

Figure 26. *Souryu-IV.*

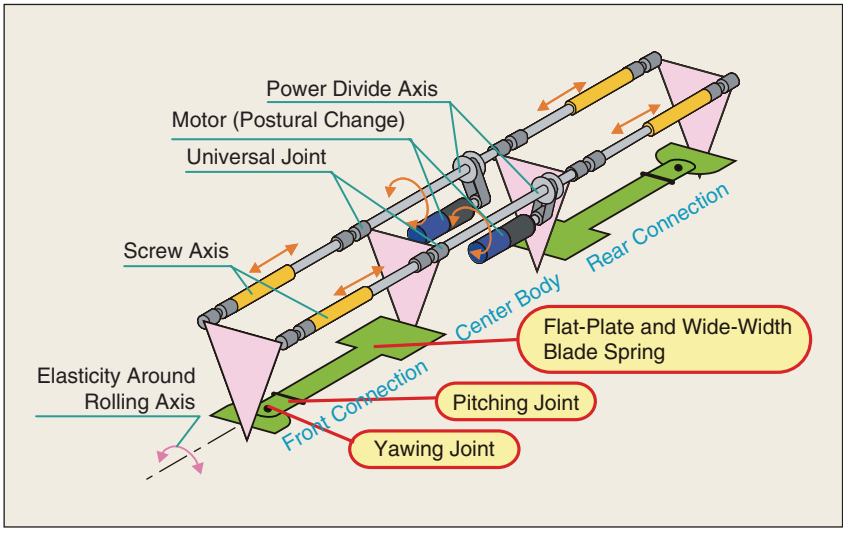

Figure 27. *Joint of Souryu-IV.*

Authorized licensed use limited to: IEEE Xplore. Downloaded on November 21,2023 at 09:26:57 UTC from IEEE Xplore. Restrictions apply.

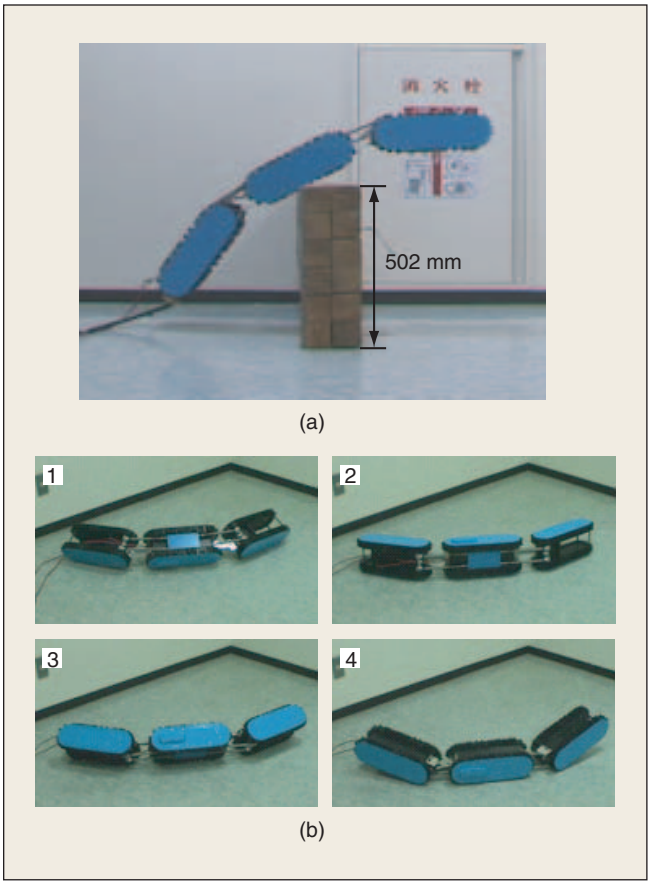

Figure 28. *Motion of Souryu-IV. (a) Climbing a step. (b) Turnover motion.*

are commonly found at disaster sites. This crawler unit is already commercialized by a company [12].

Conclusions

In this article, we have introduced the biomechanical research on snakes and developmental research on snake-like robots that we have been working on. We could not introduce everything we developed. There were also a smaller snake-like active endoscope [13]; a large-sized snake-like inspection robot for nuclear reactor related facility, Koryu [14], 1 m in height, 3.5 m in length, and 350 kg in weight; and several other snake-like robots.

Development of snake-like robots is still one of our latest research topics. We feel that the technical difficulties in putting snake-like robots into practice have almost been overcome by past research, so we believe that such practical use of snake-like robots can be realized soon.

Acknowledgment

We would like to express our gratitude to the excellent students of Tokyo Institute of Technology, who cooperated with these research projects.

Keywords

Biologically inspired robot, snake-like robot, mechanical design.

References

[1] S. Hirose, *Biologically Inspired Robots*. London, U.K.: Oxford Univ. Press, 1993.

[2] H. Yamada and S. Hirose, "Study of active cord mechanism—Generalized basic equations of the locomotive dynamics of the ACM and analysis of sinus-lifting," (in Japanese), *J. Robot. Soc. Jpn.*, vol. 26, no. 7, pp. 801–811, 2008.

[3] M. Mori, S. Hirose, "Three-dimensional serpentine motion and lateral rolling by active cord mechanism ACM-R3," in *Proc. 2002 IEEE/RSJ Int. Conf. Intelligent Robots and Systems*, 2002, pp. 829–834.

[4] C. Wright, A. Johnson, A. Peck, Z. McCord, A. Naaktgeboren, P. Gianfortoni, M. Gonzales-Rivero, R. Hatton, H. Choset, "Design of modular snake robot," in *Proc. IEEE Int. Conf. Intelligent Robots and Systems*, 2007, pp. 2609–2614.

[5] H. Yamada, S. Chigisaki, M. Mori, K. Takita, K. Ogami, S. Hirose, "Development of amphibious snake-like robot ACM-R5," in *Proc. 36th Int. Symp. Robotics*, TH3C4, 2005.

[6] T. Takayama, S. Hirose, "Amphibious 3D active cord mechanism "HELIX" with helical swimming motion," in *Proc. IEEE Int. Conf. Intelligent Robots and Systems*, 2002, vol. 1, pp. 775–780.

[7] H. Ohno, S. Hirose, "Design of Slim Slime robot and its gait of locomotion," in *Proc. 2001 IEEE/RSJ Int. Conf. Intelligent Robots and Systems*, pp. 707–715.

[8] S. Sugita, K. Ogami, M. Guarnieri, S. Hirose, K. Takita, "A study on the mechanism and locomotion strategy for new snake-like robot active cord mechanism—Slime model 1 ACM-S1," *J. Robot. Mechatron.*, vol. 20, no. 2, pp. 302–310, 2008.

[9] H. Yamada, S. Hirose, "Development of practical 3-dimensional active cord mechanism ACM-R4," *J. Robot. Mechatron.*, vol. 18, no. 3, pp. 305–310, 2006.

[10] H. Kimura, S. Hirose, "Development of Genbu: Active wheel passive joint articulated mobile robot," in *Proc. 2002 IEEE/RSJ Int. Conf. Intelligent Robots and Systems*, 2002, pp. 823–828.

[11] M. Arai, Y. Tanaka, S. Hirose, H. Kuwahara, S. Tsukui, "Development of "Souryu-IV" and "Souryu-V": Serially connected crawler vehicles for in-rubble searching operations," *J. Field Robot.*, vol. 25, no. 1–2, pp. 31–65, 2008.

[12] Crawler Robot Department, TOPY Industries. [Online]. Available: http://www.topy.co.jp/english/dept/bdp/index.html

[13] S. Hirose, K. Ikuta, M. Tsukamoto, "Development of shape memory alloy actuator. Measurement of material characteristics and development of active endoscopes," *Adv. Robot.*, vol. 4, no. 1, pp. 3–27, 1990.

[14] E. F. Fukushima, S. Hirose, "An efficient steering control formulation for the articulated body mobile robot "KR-II"," *Autonom. Robots*, vol. 3, no. 1, pp. 7–18, 1996.

Shigeo Hirose received his doctoral degree in control engineering from Tokyo Institute of Technology in 1976. His research interests lie in the design and control of snake-like robots, walking robots, wheels and crawler vehicles, omnidirectional robots, wall climbing robots, planetary exploration robots, and devices for control of robots. He received Pioneer in Robotics and Automation Award from IEEE Robotics and Automation Society in 1999. He is a fellow of IEEE.

Hiroya Yamada received his doctoral degree in mechanical and aerospace engineering from Tokyo Institute of Technology in 2008. He is a member of IEEE. His research interests lie in the area of biologically inspired robots.

Address for Correspondence: Shigeo Hirose, Department of Mechanical and Aerospace Engineering, Tokyo Institute of Technology, 2-12-1 Ookayama, Meguro-ku, Tokyo, 152-8552, Japan. E-mail: hirose@mes.titech.ac.jp.

Authorized licensed use limited to: IEEE Xplore. Downloaded on November 21,2023 at 09:26:57 UTC from IEEE Xplore. Restrictions apply.